Osteoarthritis and Cartilage 27 (2019) 336–346

Osteoarthritis and Cartilage

MiR-15b is a key regulator of proliferation and apoptosis of chondrocytes from patients with condylar hyperplasia by targeting IGF1, IGF1R and BCL2

P. Cao † [a], Y. Feng † [a], M. Deng ‡, J. Li ‡, H. Cai ‡, Q. Meng ‡, W. Fang ‡, Y. Li ‡, J. Ke † [**], X. Long ‡ [*]

† State Key Laboratory Breeding Base of Basic Science of Stomatology (Hubei-MOST) & Key Laboratory of Oral Biomedicine Ministry of Education (KLOBM), School and Hospital of Stomatology, Wuhan University, Wuhan, Hubei Province, China
‡ Department of Oral and Maxillofacial Surgery, School and Hospital of Stomatology, Wuhan University, Wuhan, Hubei province, China

ARTICLE INFO

Article history:
Received 4 April 2018
Accepted 13 September 2018

Keywords:
MiR-15b
Condylar hyperplasia
IGF1
IGF1R
BCL2

SUMMARY

Objective: This study aimed to explore potential microRNAs (miRNAs), which participate in the pathological process of condylar hyperplasia (CH) through targeting specific proliferation- and apoptosis-related genes of chondrocytes.

Methods: Insulin-like growth factor 1 (IGF1), IGF1 receptor (IGF1R) and B-cell CLL/lymphoma 2 (BCL2) in CH cartilage were detected by real-time polymerase chain reaction (PCR), Western blot, immunohistochemistry and immunofluorescence. MiRanda and TargetScanS algorithms were used to predict certain miRNAs in CH chondrocytes concurrently modulating the above three genes. MiR-15b was screened and identified using real-time PCR. After transfection of miR-15b mimics or inhibitor into CH chondrocytes, expression of the above three genes was detected by real-time PCR and western blot, meanwhile, cell proliferation and apoptosis was examined by CCK8, cell cycle assays, flow cytometry and Hoechst staining. Dual luciferase activity was performed to identify the direct regulation of miR-15b on IGF1, IGF1R and BCL2.

Results: Expression of IGF1, IGF1R and BCL2 increased in CH cartilage. Seven microRNAs concurrently correlated with IGF1, IGF1R and BCL2. Among them, only miR-15b significantly changed in CH chondrocytes. Overexpression of miR-15b in CH chondrocytes suppressed the expression of IGF1, IGF1R and BCL2, while it increased when miR-15b was knockdown. Furthermore, miR-15b suppressed their expression by directly binding to its 3′-UTR in these cells. Besides, miR-15b hampered chondrocytes proliferation through targeting IGF1 and IGF1R and accelerated chondrocytes apoptosis through targeting BCL2.

Conclusion: Suppressed miR-15b contributed to enhanced proliferation capacity and weakened apoptosis of chondrocytes through augmentation of IGF1, IGF1R and BCL2, thereby resulting in development of CH.

Introduction

Condylar hyperplasia (CH) is a progressive and pathologic overgrown disease in temporomandibular joint (TMJ) of human, which frequently occurred unilaterally in the early age of people and resulted in occlusal disturbance or self-limiting facial asymmetry[1,2]. The etiology and pathology of CH is uncertain with the characteristics of progressive growth in one of the human mandibular condyles after the opposite condyle stopped grown[3,4]. The golden standard for the clinical diagnosis of CH is Single-

* Address correspondence and reprint requests to: X. Long, Department of Oral and Maxillofacial Surgery, School and Hospital of Stomatology, Wuhan University, 237 Luoyu Road, Wuhan, Hubei province, 430079, China.
** Address correspondence and reprint requests to: J. Ke, State Key Laboratory Breeding Base of Basic Science of Stomatology (Hubei-MOST) & Key Laboratory of Oral Biomedicine Ministry of Education (KLOBM), School and Hospital of Stomatology, Wuhan University, Wuhan, Hubei Province, 430079, China.
E-mail addresses: kejin@whu.edu.cn (J. Ke), longxing@whu.edu.cn (X. Long).
[a] Pinyin Cao and Yaping Feng contributed equally in this article.

https://doi.org/10.1016/j.joca.2018.09.010
1063-4584/

photon emission computed tomography (SPECT) bone scintigraphy[3].

Our previous studies have demonstrated abnormally enhanced proliferation of chondrocytes as well as matrix synthesis contributes to CH development[1]. Insulin-like growth factor 1 (IGF1), as a critical proliferation inducer, boosts CH development by fortifying the proliferation capacity of chondrocytes through IGF1R[1]. Besides, the widely accepted notion related to maintaining normal function and morphology of articular cartilage focuses on the dynamic balance of chondrocytes proliferation and apoptosis. Therefore, it is reasonable to assume that CH, recognized as a pathological cartilage disease, not only displays chondrocytes over-proliferation, but also initiates abnormal cell apoptosis. B-cell CLL/lymphoma 2(BCL2) is a primary anti-apoptotic factor in its family, which expresses in various cell types, including human umbilical vein endothelial cells, acute myeloid leukemia cells and osteoblastic cells[5–11]. Recent study has demonstrated in osteoarthritis, the enhanced chondrocytes apoptosis was correlated with attenuated expression of BCL2, indicating BCL2 can affect chondrocytes apoptosis[7]. Nevertheless, whether BCL2 abnormally expresses in CH chondrocytes remains unclear.

MicroRNAs (miRNAs) are a quantity of endogenous, small non-coding RNAs of 21–25nt, which play important roles in varieties of biological processes[12]. One of functions for miRNAs is to modulate cell proliferation and apoptosis[13]. In human cervical cancer cells, miR-497 targeted RAF-1 to induce cell apoptosis and decreased cell proliferation via MAPK/ERK signaling pathway[14]. MiR-129 increased proliferation and decreased apoptosis of hippocampal neurons in rats by targeting gene c-Fos through the MAPK signaling pathway[15]. Recent attention has switched to exploring the relationship between miRNAs and chondrocytes proliferation as well as apoptosis. MiR-337-3p regulated chondrocytes proliferation and apoptosis in osteoarthritis through PTEN/AKT axis[16]. Overexpression of miR-24 could promote chondrocytes proliferation and suppress chondrocytes apoptosis by targeting C-myc through preventing the MAPK signaling pathway[17]. However, based on our knowledge, there is no study exploring function of certain miRNAs in the proliferation and apoptosis of chondrocytes from patient with CH.

The present study was aimed to detect whether the aberrant expression of IGF1, IGF1R and BCL2 occurs in CH tissue and to screen specific miRNAs responsible for regulating the above three proteins concurrently in CH chondrocytes. Additionally, the function of the selected miRNAs in modulating the proliferation and apoptosis of these cells was also investigated.

Materials and methods

Samples collection and cell culture

The condyle cartilage specimens of condylar hyperplasia (CH) were obtained from 15 patients (male: 5, female: 10; age (mean): 18–30 (23.5)) with the surgery of condylectomy in the School and Hospital of Stomatology, Wuhan University. All the patients were diagnosed according to SPECT and confirmed growth activity in the affected lateral condyle. CH cartilage sample was collected from the upper portion of the condyle, which was 5–6 mm of the condyle from the medial to the lateral pole as other previous study shown [18]. nine samples (male: 5, female: 4; age (mean): 18–30 (25.3)) from sagittal fracture of condyle were considered as normal, as they were at a certain distance from the fracture line. Furthermore, these samples were verified as normal under microscopy using hematoxylin and eosin staining, which has been demonstrated in our previous study [1,4]. The experimental protocol was approved by the Human Research Ethics Committee, School and Hospital of Stomatology, Wuhan University, and written consent was obtained from all patients included in this study (see Appendix 1).

RNA extraction and quantitative real-time RT-PCR (qRT-PCR)

Total RNA from in articular cartilage samples and cultured cells was isolated using the Trizol (Takara, Otsu, Japan). Reverse transcription of Miribonucleic acid (RNA) and mRNA were performed using Mir-X miRNA First-Strand Synthesis Kit (Tailing Reaction, Takara, Otsu, Japan) and PrimeScript Reverse Transcriptase (Takara, Otsu, Japan) according to the manufacturer's protocol, respectively. ABI Prism 7500 Real-time polymerase chain reaction (PCR) System (Applied Biosystems, Foster City, CA, USA) with Mir-X miRNA qRT-PCR SYBR Kit (Takara, Otsu, Japan) or PrimeScript RT reagent kit using gDNA Eraser (TaKaRa, Dalian, China) was used to perform the qRT-PCR reactions, respectively. U6 and β-actin were used to normalize mRNA and miRNA level respectively. Expression of relative genes was calculated using the cycle threshold method ($2^{-\Delta\Delta Ct}$) method. The primers used were shown in Table I.

Western blot analysis

The protein levels of IGF1, IGF1R and BCL2 in articular cartilage samples and cultured cells were detected by western blot. MPER Mammalian Protein Extraction Reagent (Thermo Scientific, Carlsbad, CA) was used to extract the protein (see Appendix 1).

Immunohistochemistry (IHC) and immunofluorescence (IF) staining

The IHC and IF staining on the condyle cartilage specimens of CH was performed using rabbit polyclonal antibody to IGF1 (ab40657, Abcam), rabbit monoclonal antibody to IGF1R (ab182408, Abcam) and mouse monoclonal antibody to BCL2 (YM3041, Immunoway). The IHC staining followed our previous study 13 (see Appendix 1).

Table I
Primer sequences of microRNA and mRNA for reverse transcription quantitative polymerase chain reaction (qRT-PCR).Note: F, forward primer; *R*, reverse primer; GSP, gene specific primer; mRQ 3′Primer from Mir-X miRNA First-Strand Synthesis Kit (Takara, Otsu, Japan). The sequence of a specific miRNA can be obtained from miRBase sequences (http://www.mirbase.org)

Gene	Primer sequence (5′-3′)
MiR-15a	GSP: 5′- TAGCAGCACATAATGGTTTGTG-3′
MiR-15b	R: mRQ 3′ Primer
MiR-16	GSP: 5′- TAGCAGCACATCATGGTTTACA-3′
MiR-195	R: mRQ 3′ Primer
MiR-424	GSP: 5′- TAGCAGCACGTAAATATTGGCG-3′
MiR-497	R: mRQ 3′ Primer
MiR-6838	GSP: 5′- TAGCAGCACAGAAATATTGGC-3′
U6	R: mRQ 3′ Primer
IGF1	GSP: 5′-CAGCAGCAATTCATGTTTTGAA-3′
IGF1R	R: mRQ 3′ Primer
BCL2	GSP: 5′- CAGCAGCACACTGTGGTTTGT-3′
β-actin	R: mRQ 3′ Primer
	GSP: 5′- AAGCAGCAGTGGCAAGACTCCT-3′
	R: mRQ 3′ Primer
	F: 5′-CTCGCTTCGGCAGCACA-3′
	R: 5′-AACGCTTCACGAATTTGCGT-3′
	F: 5′- TCTTCAGTTCGTGTGTGGAGACAG-3′
	R: 5′- GGGTGCGCAATACATCTCCAG-3′
	F: 5′- CTGAAAGGAAGCGGAGAGATG-3′
	R: 5′- GCAAAGACGAAGTTGGAGGC-3′
	F: 5′- TGGACAACCATGACCTTGGAC-3′
	R: 5′- GTGCTCAGCTTGGTATGCAGAA-3′
	F: 5′- TGGCACCCAGCACAATGAA-3′
	R: 5′- CTAAGTCATAGTCCGCCTAGAAGCA-3′

Cell transfection

Chondrocytes transfected with miR-15b mimics, inhibitor, negative control, inhibitor negative control or siRNA (50 nM) (GenePharma, Shanghai, China) by GenMuteTM small interfering RNA (siRNA) & deoxyribonucleic acid (DNA) Transfection Reagent (SignaGen, Rockville, MD, USA) according to manufacturer's protocols (see Appendix 1).

Luciferase report assay

The reporter plasmid containing 485bp of the 3' -untranslated regions (3′-UTR) of human IGF1 mRNA, 487bp of the 3' -untranslated regions (3′-UTR) of human IGF1R mRNA or 482bp of the 3′-untranslated regions (3′-UTR) of human BCL2 mRNA was constructed by the p-EZX-MT01 miRNA expression reporter vector system (GeneCopoeia, USA). The nucleotide sequence complementary of mature miR15b-5p seed sequence (ACAUUUGGUACUACACGACGAU) was included in three reporter plasmids. The nucleotide sequence complementary to miR15b-5p was changed in the mutant plasmid. The 3′-UTR of integrated with firefly luciferase (hLuc) and the internal reference was renilla luciferase (hRLuc). Chondrocytes transfected with 0.5μg of reporter plasmid and 50 nM miRNA mimics or negative control using GenMute (SignaGen, USA) according to manufacturer's protocols in every single well of 6-well plate. The transfection efficiency was maintained at a level around 80% by fluorescence observation in control group, which was shown in Appendix 2. After 48 h of transfection, luciferase activity assay was carried out by Luc-Pair ™ Duo-Luciferase Assay Kit 2.0 (GeneCopoeia, USA) and using GloMax 20/20 LUMINOMETER (promega, USA) to measure fluorescence. Firefly luciferase activity was normalized to Renilla luciferase activity.

Proliferation assay (cell cycle assay and cck8)

When the percentage of cell reached about 80%, cells were washed with phosphate buffer saline (PBS) twice. Digested the cells by 0.25% trypsin, then seeded the cells to a 96-well plate with 3 × 103-6 × 103 cells in each well (see Appendix 1).

Apoptosis assay

Cell apoptosis analysis was performed according to the manufacturer's instructions by Annexin-VFITC Apoptosis Detection Kit (BD, USA). Chondrocytes were transfected with miR-15b-5p mimics, miR-15b-5p inhibitor and miR-15b-5p negative control when the percentage of cells grown to 70–90%. After transfection, cells were incubated at 37°C for 48 h. Then the Annexin V/fluorescein isothiocyanate Apoptosis Detection kit was used to stain the cells (see Appendix 1).

Statistical analysis

All data were analyzed using Prism 5.0 (Graphpad software, San Diego, California, USA). All quantitative data were presented as the means and 95% confidence intervals (CIs). Non-parametric Mann–Whitney *U* test was used for two independent groups. For the data of luciferase report assay, one-way analysis of variance (ANOVA) with Tukey's *post hoc* analysis was used for multi-comparisons after confirmation of data fulfilling normal distribution and homogeneity of variances. $P < 0.05$ was considered statistically significant.

Results

Up-regulated expression of IGF1, IGF1R and BCL2 in CH cartilage

As shown in Fig. 1(A), the expression of IGF1, IGF1R and BCL2 mRNA in CH was about 3 -fold, 4 –fold and 4.5 -fold higher than that in the control group, respectively. Similarly, our western blotting results also exhibited that the expression of IGF1, IGF1R and BCL2 in CH cartilage was about 13-fold, 8-fold and 2-fold higher compared with the control group [Fig. 1(B)]. Likewise, the

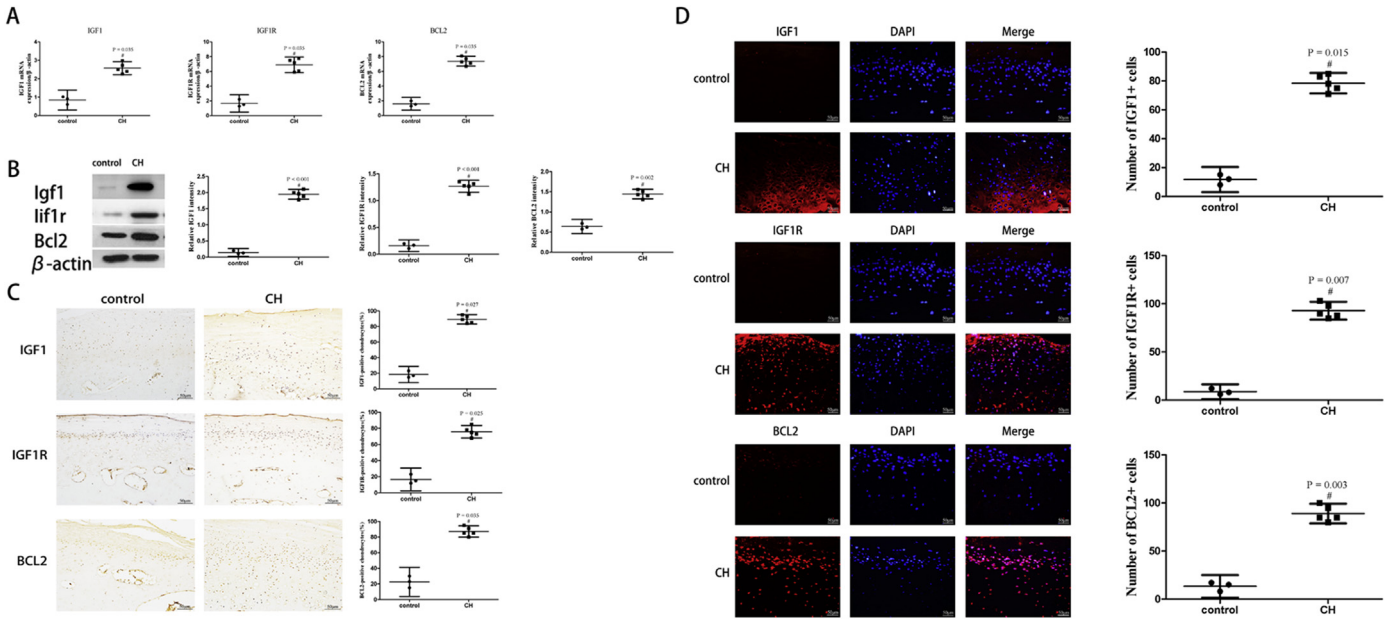

Fig. 1. Up-regulated expression of IGF1, IGF1R and BCL2 in CH cartilage. (A) The mRNA and protein expression levels of IGF1, IGF1R and BCL2 in CH cartilage were detected by qRT-PCR (A) and Western blot (B). β-actin served as an internal control. [five CHs (two males, three females; mean age: 24.5), three controls (two males, one female; mean age: 23.6)]. (C, D) Immunohistochemistry (IHC) and immunofluorescence (IF) staining of IGF1, IGF1R and BCL2 in condyle cartilage of CH group and control group. [five CHs (two males, three females; mean age: 24.5), three controls (two males, one female; mean age: 23.6)], three controls (one male, two females; mean age: 25.8)]. Each dot represents a mean value from triplicate of one donor and horizontal lines indicate the mean and 95% CIs of the values from different donors per group. Data were analyzed using Mann–Whitney *U* test. *P*-values were calculated compared to the control group.

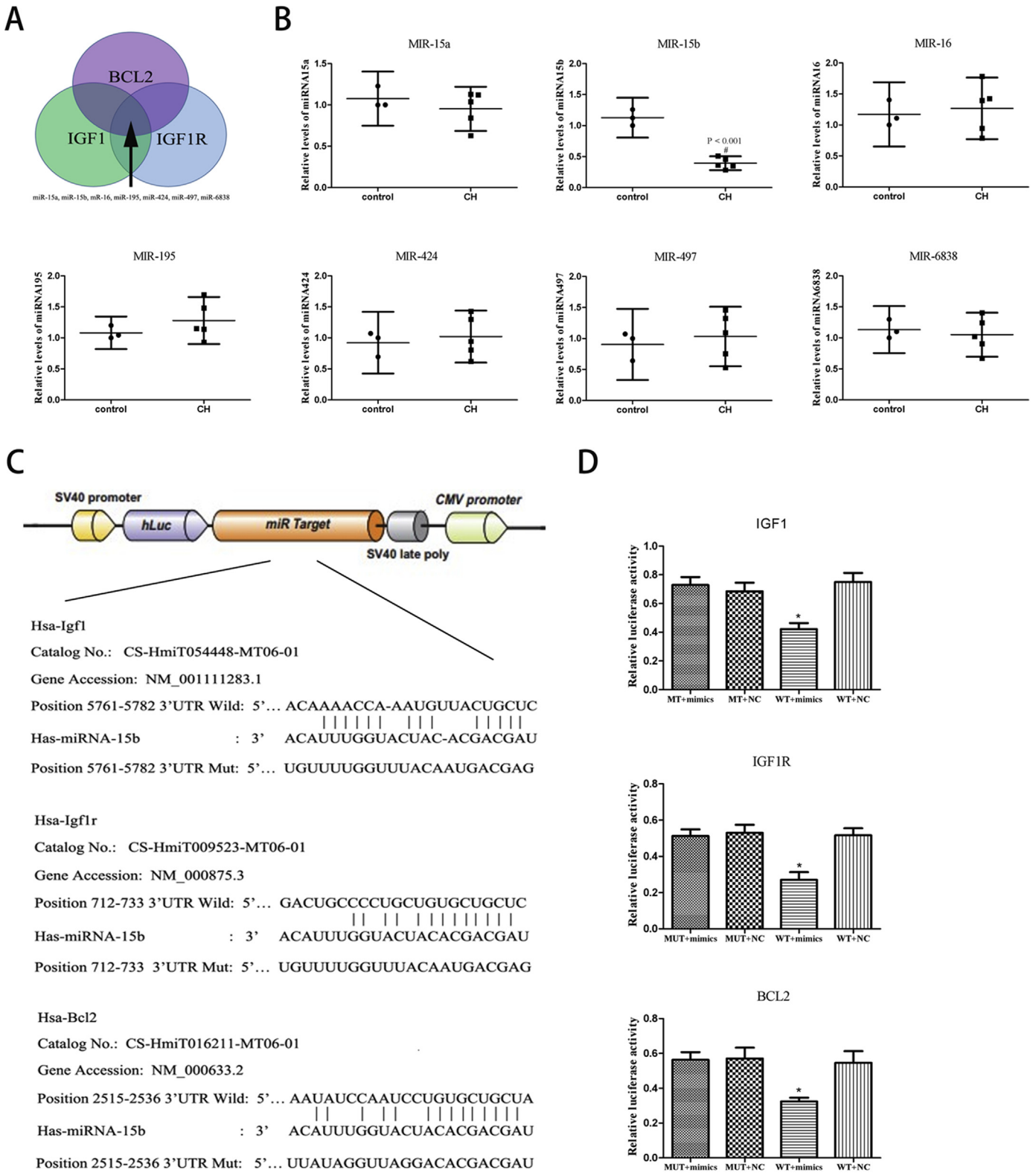

Fig. 2. Prediction and identification of microRNAs related to IGF1, IGF1R and BCL2 and confirmation of IGF1, IGF1R and BCL2 as the direct targets of miR-15b in CH chondrocytes. (A) MiR-15a, miR-15b, mR-16, miR-195, miR-424, miR-497 and miR-6838 were the prediction of microRNAs concurrently correlated with IGF1, IGF1R and BCL2 using TargetScan. (B) The expression of miR-15b was the only one significantly changed in CH chondrocytes detected by qRT-PCR. [five CHs (two males, three females; mean age: 24.5), three controls (two males, one female; mean age: 23.6)]. Each dot represents a mean value from triplicate of one donor and horizontal lines indicate the mean and 95% CIs of the values from different donors per group. Data were analyzed using Mann–Whitney *U* test. *P*-values were calculated compared to the control group. (C) IGF1, IGF1R and BCL2 have the same conserved binding sites with miR-15b. (D) Dual luciferase assay was performed in chondrocytes, which were transfected with luciferase construct with miR-15b mimics or mimics control. Relative luciferase activity was significantly reduced in WT + mimics group compared with other groups. Values were shown as mean ± SD of $n = 5$ and analyzed using one-way ANOVA test. $^{*}P < 0.05$. MT, mutant; WT, wild type; NC, negative control.

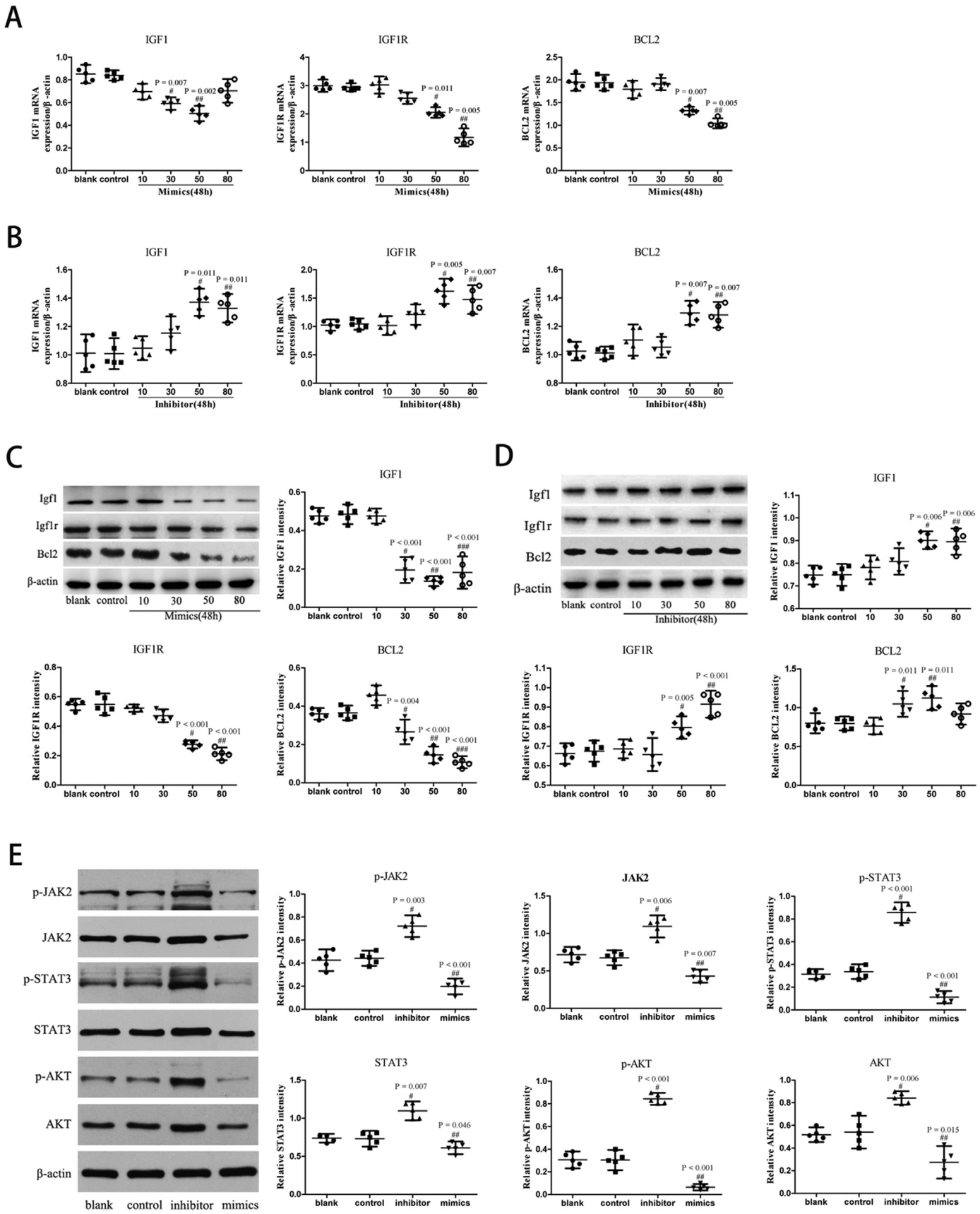

Fig. 3. Negative correlation between IGF1, IGF1R, BCL2 and miR-15b in CH chondrocytes. (A, B) QRT-PCR was used to detect the effects of different concentration of miR-15b mimics or inhibitor on mRNA expression of IGF1, IGF1R and BCL2 after the transfection of 48 h. (C, D) Western blot was used to detect the protein level of IGF1, IGF1R and BCL2 with different concentration of miR-15b mimics or inhibitor after the transfection of 48 h. (E) Western blot was used to detect the protein level of JAK2, p-JAK2, STAT3, p-STAT3, AKT, p-

immunohistochemistry (IHC) and immunofluorescence (IF) staining results revealed that the expression of IGF1, IGF1R and BCL2 were much higher in CH cartilage compared with the control group. The expression of IGF1, IGF1R and BCL2 mainly distributed in the proliferative and hypertrophic zones [Fig. 1(B) and (D)].

Prediction and identification of microRNAs related to IGF1, IGF1R and BCL2 in CH chondrocytes

We used TargetScan (http://www.targetscan.org/) and miRBase (http://www.mirbase.org/) to find the possible microRNAs related to IGF1, IGF1R and BCL2 in CH chondrocytes. As shown in Fig. 2(A), seven microRNAs, including miR-15a, miR-15b, mR-16, miR-195, miR-424, miR-497, and miR-6838 were screened out. Among them, miR-15b was the only one changed in CH chondrocytes through real time PCR (Fig. 2(B), $P < 0.001$). MiR-15b was currently reported to play a crucial role in various cells proliferation and apoptosis[11,19–22]. Hence, it was reasonable for us to assume miR-15b regulated the proliferation and apoptosis of CH chondrocytes by targeting at IGF1, IGF1R and BCL2 genes.

Confirmation of IGF1, IGF1R and BCL2 as the direct targets of miR-15b in CH chondrocytes

To verify the direct effect of miR-15b on IGF1, IGF1R and BCL2 transcripts, IGF1, IGF1R and BCL2 3′-UTR/mutant reporter systems [Fig. 2(C)] were constructed and transiently transfected into chondrocytes accompanied with miR-15b mimics or negative control. As shown in Fig. 2(D), with the over-expression of miR-15b, the luciferase activity of IGF1,IGF1R and BCL2 in WT + mimics group was evidently reduced as compared with MUT + mimics group [mean differences (MD) 0.3, 95% confidence interval (95% CI) 0.09 to 0.52, IGF1; 0.24, 0.08 to 0.40, IGF1R; 0.24, 0.04 to 0.44, BCL2], MUT + NC group (MD 0.26, 95% CI 0.05 to 0.48, IGF1; 0.25, 0.10 to 0.41 IGF1R; 0.25, 0.09 to 0.40, BCL2) and WT + NC group (MD 0.33, 95% CI 0.11 to 0.54, IGF1; 0.25, 0.09 to 0.40, IGF1R; 0.22, 0.02 to 0.42, BCL2). These results illustrated that suppression of IGF1, IGF1R and BCL2 was due to miR-15b in CH chondrocytes directly binding to the complementary seed sequence in 3′-UTR of IGF1, IGF1R and BCL.

Negative regulation between IGF1, IGF1R, BCL2 and miR-15b in CH chondrocytes

As shown in Fig. 3(A), the mRNA expression of IGR1, IGF1R and BCL2 decreased evidently with the concentration of 50 nM transfection of miR-15b mimics in CH chondrocytes after 48 h compared with that from the negative control. Likewise, with the concentration of 50 nM transfection of miR-15b inhibitor after 48 h, the mRNA expression of IGF1, IGF1R and BCL2 increased significantly compared with that from the negative control [Fig. 3(B)]. Recent study has demonstrated that miR-15b could suppress targeted genes through not only ruining stability of mRNAs, but also inhibiting the translation of transcripts[23]. Hence, it is necessary to investigate the production of the above three factors after transfection of miR-15b mimics or inhibitor. Our western blot results revealed that the protein level of IGF1, IGF1R and BCL2 in CH chondrocytes reduced evidently after transfection with 50 nM mimics compared with that from the negative control [Fig. 3(C)]. Consistently, after transfection of 50 nM inhibitor, the protein level of IGF1, IGF1R and BCL2 increased compared with the negative control group [Fig. 3(D)]. Taken together, miR-15b negatively regulated expression of IGF1, IGF1R and BCL2 both on mRNA level and protein level. Concentration at 50 nM transfection for either miR-15b mimics or inhibitor was optimal and utilized for the subsequent experiments.

In addition to the direct regulation of miR-15b on IGF1, IGF1R and BCL2 in CH chondrocytes, whether the indirect regulation exists or not needed to be addressed. JAK/STAT and PI3K/AKT are classical signal pathways for BCL2 and IGF1/IGF1R, individually[24,25]. Hence, whether miR-15b was able to modulate the expression of JAK/STAT and PI3K/AKT in these cells was investigated. As shown in Fig. 3(E), the protein levels of JAK2, p-JAK2, STAT3, p-STAT3, AKT, p-AKT significantly increased after transfection of 50 nM miR-15b inhibitor, while decreased when 50 nM miR-15b mimics was transfected compared with the negative control group.

MiR-15b affects CH chondrocytes proliferation and apoptosis through regulation of IGF1, IGF1R and BCL2

The CCK8 assay results shown that CH chondrocytes after transfection of miR-15b mimics revealed lower cell proliferation rate ($P = 0.007$), while when cell transfected with miR-15b inhibitor, the proliferation rate increased compared with the negative control [Fig. 4(A), $P = 0.015$]. To investigate whether IGF1 is directly responsible for CH chondrocytes proliferation, IGF1 siRNA was used to knock down the expression of IGF1. The protein level of IGF1 evidently decreased after transfection of IGF1 siRNA, which was shown in Appendix 3. Silencing of IGF1 expression after transfection of miR-15b inhibitor in CH chondrocytes significantly decreased cell proliferation [Fig. 4(A)]. Subsequently, our cell cycle analysis results showed that in the control group, the ratio of CH chondrocytes at S stage was 9.78%, while the ratio was increased to 11.2% in the miR-15b inhibitor group, and decreased to 6.78% in the mimics group [Fig. 4(B)]. These data suggested that miR-15b negatively modulates CH chondrocytes proliferation through targeting IGF1 and IGF1R.

Under a microscope, the shape of morphologic change from multiple angle or shuttle to spherical could be detected at 24 h after transfection of miR-15b mimics in CH chondrocytes [Fig. 4(C)]. Under a fluorescence microscope, transfected with miR-15b mimics, cells presented shrunken nuclei and condensed chromatin, which were the typical apoptotic morphological changes. In contrast, when cells were transfected with miR-15b inhibitor, less apoptotic morphological changes was found compared with the negative control [Fig. 4(C)]. As shown in Fig. 4(D), cells exposure to the miR-15b mimics increased the rate of apoptosis. On the contrary, cells exposure to the miR-15b inhibitor decreased the rate of apoptosis compared with the group transfected with negative microRNAs. These findings indicated that miR-15b contributes to apoptosis of CH chondrocytes. Caspases, proteases of BCL2 downstream, are crucial stimulator of cell apoptosis[23,26,27]. Among them, caspase 3 is a frequently activated apoptosis protease[27]. Interestingly, the expression of caspase 3 and activated caspase 3 in CH chondrocytes remained constant regardless of BCL2 expression was down-regulated or augmented after transfection of miR-15b mimics or inhibitor [Fig. 4(E)]. Fas is a member of the tumor

AKT with the concentration of 50 nM miR-15b mimics or inhibitor after the transfection of 48 h. Blank, without transfection; control, transfection with negative control of miRNA. Each dot represents a mean value from triplicate of one donor and horizontal lines indicate the mean and 95% CIs of the values from different donors per group. Data were analyzed using Mann–Whitney *U* test ($n = 5$ patients, two males, three females; mean age: 24.5). *P*-values were calculated compared to the control group.

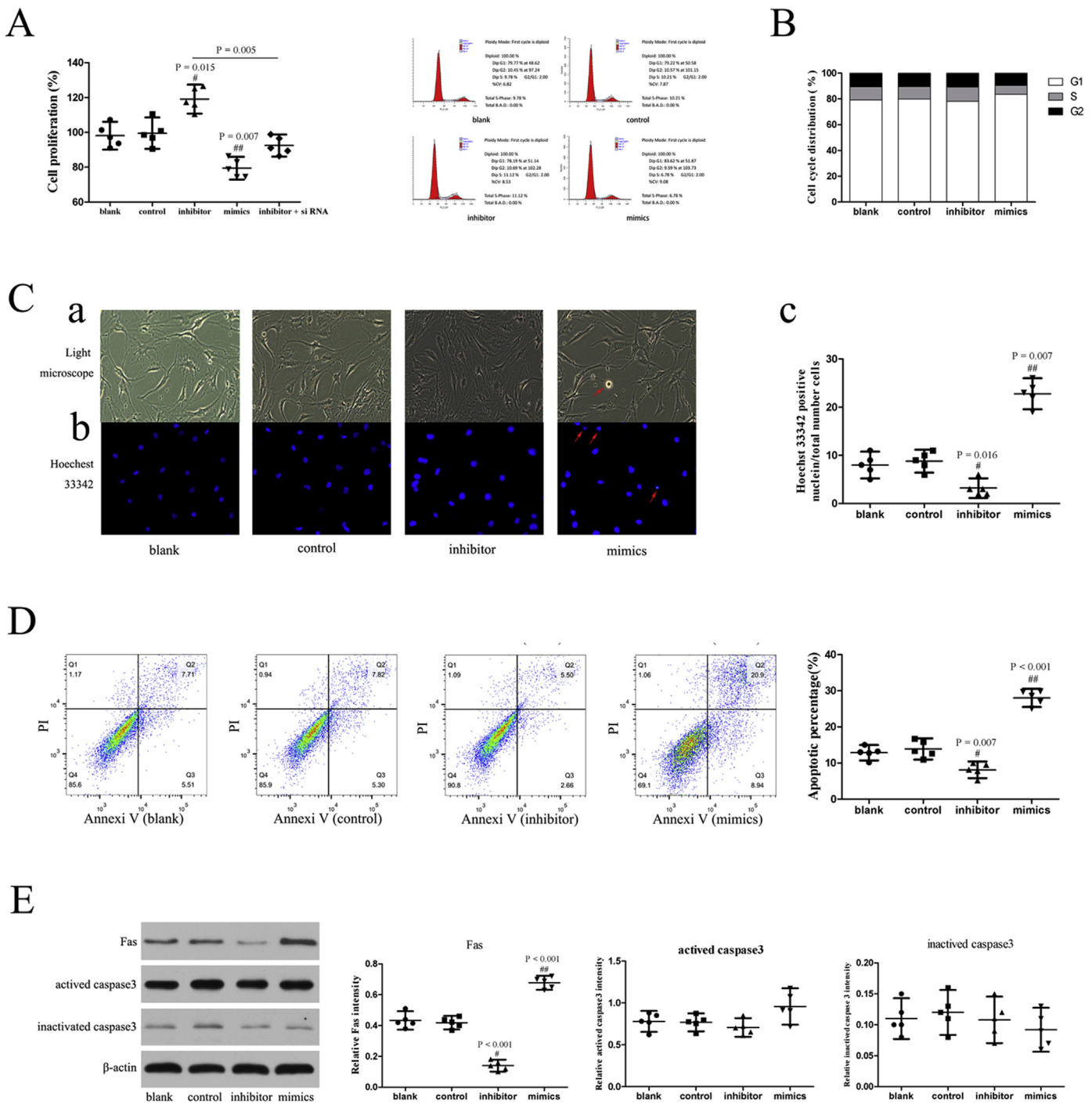

Fig. 4. MiR-15b affects CH chondrocytes proliferation and apoptosis through regulation of IGF1, IGF1R and BCL2. (A) CCK8 assay was used to measure cell proliferation. (B) Cell cycle profiles of chondrocytes transfected with miR-15b mimics, inhibitor, negative control and inhibitor+siRNA after 48 h. The shape of morphological changes were being discovered under light microscope (C a) and typical apoptotic morphological changes were detected by of Hoechst 33,342 staining under fluorescence microscope (C b). Apoptotic rate is determined by comparing the number of apoptotic cells to the total cells (C). Scale bar = 50μm. (D) Cell apoptosis ratio was being investigated by flow cytometry after the transfection of miR-15b mimics, inhibitor and negative control after 48 h. (E) Western blot was used to detect the expression of Fas, inactivated caspase 3 and actived caspase 3 in miR-15b mimics, inhibitor, negative control and bank without miRNA group. Blank, without transfection; control, transfection with negative control of miRNA. Each dot represents a mean value from triplicate of one donor and horizontal lines indicate the mean and 95% CIs of the values from different donors per group. Data were analyzed using Mann–Whitney *U* test. ($n = 5$ patients, two males, three females; mean age: 24.5). *P*-values were calculated compared to the control group.

necrosis factor (TNF)-receptor and TNF family, which could initiate cell apoptosis[28]. As shown in Fig. 4(E), the protein level of Fas significantly increased after transfection of miR-15b mimics, and evidently decreased after transfection of miR-15b inhibitor.

Discussion

In the present study, substantial expression of IGF1 and IGF1R was detected in the proliferative and hypertrophic zones of CH

cartilage, while only sporadic expression of IGF1 and IGF1R in the proliferative zone of the condylar cartilage in control groups. Consistently, a classical study on the growth plate development of rat has demonstrated that IGF1 abundantly expressed in proliferative and hypertrophic zones. They suggested that IGF1 stimulates metatarsal longitudinal growth by increasing the proportion of proliferating cells in proliferative zone and enhancing of cell differentiation/hypertrophy in hypertrophic zone[29]. Likewise, during the process of cartilage degeneration, the expression of IGF1and IGF1R decreased in proliferative and hypertrophic zones in female Sprague–Dawley rats[30]. BCL2, as a predominant anti-apoptotic factor, was frequently used as a maker of cell survival by blocking apoptosis[9]. Our results exhibited that the up-regulated expression of BCL2 was detected in the proliferative and hypertrophic zones of CH cartilage as compared with that of control group. Similarly, *Kinkel et al.* found that in the stage of growth and development of C57BL/6 mice, Bcl-2-positive chondrocytes was also found in the proliferative and hypertrophic zones[31]. Thus, our results indicating BCL2 probably promotes cartilage overgrowth of CH by suppressing chondrocytes apoptosis. Based on our knowledge, this is the first time to demonstrate the abnormally high expression of BCL2 in CH cartilage.

In our study, using miRanda and TargetScanS algorithms, we found out seven microRNAs, including miR-15a, miR-15b, mR-16, miR-195, miR-424, miR-497, miR-6838, which concurrently correlated with IGF1, IGF1R and BCL2. Among them, the expression of miR-15b was the only one significantly changed in CH chondrocytes. MiR-15b, located at 3q25.33, has significant roles in cell apoptosis, proliferation, angiogenesis, metastasis and maintaining genome stability[32]. Previous work in B-cell chronic lymphocytic leukemia has demonstrated B cells proliferation and apoptotic is connected with the expression of IGF1R, which is regulated by miR-15b[33]. BCL2 has also been verified as a direct target of miR-15b in participating of rat hepatic stellate cell apoptosis[26]. However, study in ovarian cancer cells has reported that less relationship was found between BCL2 and miR-15b in the process of ovarian proliferation[34]. This can be explained by that miR-15b may regulate cell proliferation and apoptosis through targeting specific genes in the corresponding cells. Hence, it was compulsory to investigate whether miR-15b can target IGF1, IGF1R and BCL2 genes in the proliferation and apoptosis of CH chondrocytes. By means of classical gain and loss expression of miR-15b, our study revealed the direct regulation of miR-15b on the expression of IGF1, IGF1R and BCL2 in CH chondrocytes. Besides, we also explored the indirect regulation of miR-15b on JAK/STAT and PI3K/AKT pathway in CH chondrocytes. Our results showed that the protein levels of JAK2, p-JAK2, STAT3, p-STAT3, AKT, p-AKT significantly increased after transfection of 50 nM miR-15b inhibitor, while decreased when 50 nM miR-15b mimics was transfected compared with the negative control group. These findings indicated miR-15b could regulate the expression of IGF1, IGF1R and BCL2 in CH chondrocytes both directly and indirectly. Moreover, our dual luciferase reporter assay illuminated that miR-15b suppressed IGF1, IGF1R and BCL2 expression by directly binding to its 3′-UTR. Subsequently, the suppression of IGF1and IGF1R in these cells when transfected with miR-15b mimics resulted in the reduction of cell proliferation using CCK8 and cell cycle assay, vice versa when transfected with miR-15b inhibitor. In addition, our Hoest33342 staining and flow cytometry results demonstrated remarkable apoptosis in CH chondrocytes when BCL2 expression was hampered after transfection of miR-15b mimics. Recent studies reported that caspase 3 has been negatively regulated by BCL2 during various cell apoptosis, including rat hepatic stellate cells, human colon cancer cells and mesenchymal stem cells[26,35,36]. Nevertheless, in the present study, the expression of caspase 3 and active caspase 3 in CH chondrocytes remained constant no matter when BCL2 expression was down- or up- regulated after transfection of miR-15b mimics or inhibitor. One of the reasons for these discrepancies might be that BCL2 regulates different caspase subtypes in different cells. *Sun et al.* reported that in dihydroartemisinin-induced apoptosis, diminished BCL2 activated caspase 9 rather than caspase 3 in gastric cancer[37]. The other reasonable explanation is that caspase 3 could be positively affected by certain genes which are targeted by miR-15b. Indeed, enhanced expression of miR-15b in a prostate cancer cell line inhibited reversion-inducing cysteine-rich protein with Kazal motifs (RECK) signal activation, thereby leading to caspase 3 reduction[38].

It should be noted that in the present study, CH chondrocytes expressed cleaved-caspase 3 and stained Annexin V positively without any stimulation. Previous study has approved that apoptosis was observed in chondrocytes cultured *in vitro*, and the percentage of apoptosis of chondrocytes could reach to 15.7%[39]. In our study, the percentage of apoptosis of chondrocytes without any stimulation is range from 10.2% to 14.5%. Therefore, the apoptosis in chondrocytes is in the normal range.

There are some limitations in the current study. Firstly, Luciferase report assay is routinely used to detect the direct binding relationship between miRNA and targeting genes. However, in order to acquire more convinced evidence for direct binding, Ago2-CLIP and CLIP-PCR will be helpful[40]. Secondly, we cannot excluded the influence of other known factors that affect on proliferation and apoptosis in chondrocytes. By now, based on our literature retrieval, the expression of BMP-2, TGF-β1, IGF1, IGF1R and IGF2 have been explored in the tissue of CH cartilage[1,2,4]. Indeed, it is worthwhile exploring whether BMP-2, TGF-β1 and IGF2 can affect CH chondrocytes proliferation and apoptosis or not. Thirdly, owing to the redundant regulation of miRNAs, it is impossible for us to exclude the possibility that certain miRNAs other than miR15b regulate cartilage overgrowth during the developing process of CH. However, it is appropriate for us to raise the notion that miR-15b is a key regulator for chondrocytes proliferation and apoptosis of during the process of CH as it can target IGF1, IGFR1 and BCL2 concurrently.

In conclusion, under CH circumstance, suppressed miR-15b boosted the expression of IGF1, IGF1R and BCL2 simultaneously, thereby resulting in enhanced proliferation capacity and weakened apoptosis of chondrocytes. Therefore, miR-15b, recognized as a key negative factor during the over-growth process of condylar cartilage, is a promising molecular target for CH treatment.

Author contributions

Dr Long and Dr Ke had full access to all of the data in the study and take responsibility for the integrity of the data and the accuracy of the data analysis.

Study design. Long, Ke.

Acquisition of data. Cao, Feng, Deng, Li, Cai, Meng, Fang, Li.

Manuscript preparation. Long, Ke, Cao.

Statistical analysis. Ke, Cao, Feng.

Conflict of interest

We declare no conflict of interest on this manuscript.

Acknowledgements

This study was supported by grants (No. 81100769, No. 81271171, No. 81470761, No. 81600889, No. 8177041189) from the National Science Foundation of China.

Appendix

Materials and methods

Samples collection and cell culture

The condyle cartilage specimens of condylar hyperplasia (CH) were obtained from 15 patients (male: 5, female: 10; age (mean): 18–30 (23.5)) with the surgery of condylectomy in the School and Hospital of Stomatology, Wuhan University. All the patients were diagnosed according to SPECT and confirmed growth activity in the affected lateral condyle. CH cartilage sample was collected from the upper portion of the condyle, which was 5–6 mm of the condyle from the medial to the lateral pole as other previous study shown. nine samples (male: 5, female: 4; age (mean): 18–30 (25.3)) from sagittal fracture of condyle were considered as normal, as they were at a certain distance from the fracture line. Furthermore, these samples were verified as normal under microscopy using hematoxylin and eosin staining, which has been demonstrated in our previous study 1,4. The experimental protocol was approved by the Human Research Ethics Committee, School and Hospital of Stomatology, Wuhan University, and written consent was obtained from all patients included in this study.

Five condyle cartilage tissues from CH and three normal condyle cartilage tissues were used for immunohistochemistry and immunofluorescence. Another five condyle cartilage tissues from CH and three normal condyle cartilage tissues were frozen in liquid nitrogen immediately and stored at −80°C for further western blot and RNA extraction and real-time polymerase chain reaction (PCR). The others of condyle cartilage specimens were washed three times with phosphate buffer saline (PBS) including 100 units/ml penicillin and 100 mg/ml streptomycin (Hyclone, Logan, Ut, USA). After that, cut the specimens into 1 mm^3 pieces and digested for 45 min at 37°C with 0.25% trypsin (HyClone, Logan, UT, USA). Then isolated the chondrocytes by type II collagenase (Roche, France) for 2 h at 37°C. After washing, cells were grown in Dulbecco's modified eagle medium (DMEM) (Hyclone, USA) supplemented with 10% fetal bovine serum (FBS, Hyclone, USA) and penicillin/streptomycin (100 U/mL, Hyclone, USA) on the condition of atmosphere containing 5% CO2. The primary and passage one chondrocytes were used for research.

RNA extraction and quantitative real-time RT-PCR (qRT-PCR)

Total RNA from in articular cartilage samples and cultured cells was isolated using the Trizol (Takara, Otsu, Japan). Reverse transcription of MiRNA and mRNA were performed using Mir-X miRNA First-Strand Synthesis Kit (Tailing Reaction, Takara, Otsu, Japan) and PrimeScript Reverse Transcriptase (Takara, Otsu, Japan) according to the manufacturer's protocol, respectively. ABI Prism 7500 Real-time PCR System (Applied Biosystems, Foster City, CA, USA) with Mir-X miRNA qRT-PCR SYBR Kit (Takara, Otsu, Japan) or PrimeScript RT reagent kit using gDNA Eraser (TaKaRa, Dalian, China) was used to perform the qRT-PCR reactions, respectively. U6 and β-actin were used to normalize mRNA and miRNA level respectively. Expression of relative genes was calculated using the cycle threshold method (2 -ΔΔCt) method. The primers used were shown in Table I.

Western blot analysis

The protein levels of IGF1, IGF1R and BCL2 in articular cartilage samples and cultured cells were detected by western blot. MPER Mammalian Protein Extraction Reagent (Thermo Scientific, Carlsbad, CA) was used to extract the protein. Equal amounts of proteins (30μg) were separated by sodium dodecyl sulfate-polyacrylamide gel electrophoresis transferred to polyvinylidene fluoride (PVDF) membranes (Millipore, MA, USA) as previously described 19. The membrane was blocked in 5% skim milk and then incubated in different primary antibodies for IGF1 (ab9572, Abcam), IGF1R (ab39675, Abcam), BCL2 (YM3041, Immunoway), caspase 3 (19,677-1-AP, Proteintech), activated caspase 3 (66,470-2-Ig, Proteintech), JAK2 (AF6022, Affbiotech), p-JAK2 (AF3023, Affbiotech), STAT3 (ab109085, Abcam), p-STAT3 (ab76315, Abcam), AKT (#4695, CST), p-AKT (#4060, CST), FAS (ab82419, Abcam) and β-actin (ab8227, Abcam) at 40C overnight. After washed in PBS, horse radish peroxide-seconjugated secondary antibodies was used to incubate for 1 h at room temperature. Positive signals were detected using electro-chemi-luminescence (ECL) reagents (Advansta, Menlo Park, CA, USA) for analysis.

Immunohistochemistry (IHC) and immunofluorescence (IF) staining

The IHC and IF staining on the condyle cartilage specimens of CH was performed using rabbit polyclonal antibody to IGF1 (ab40657, Abcam), rabbit monoclonal antibody to IGF1R (ab182408, Abcam) and mouse monoclonal antibody to BCL2 (YM3041, Immunoway). The IHC staining followed our previous study 13. For IF staining, the sections were incubated with 0.4% pepsin (Maixin, Fuzhou, China) for 30 min at 370C, and then incubated with 1% bull serum albumin (BSA) for 1 h. The sections were incubated with anti-IGF1, anti-IGF1R or anti-BCL2 antibody at 40C overnight in a humidified chamber. The sections were then reacted with secondary antibodies conjugated with fluorescence for 30 min at 37°C with the nuclei staining by 4′,6-diamidino-2-phenylindole (DAPI). And then observed the reactivity under light microscopy or a fluorescence microscope (Leica, Wetzlar, Germany). When the control and CH group were compared, we normalized by the number of cells. The number of positive cells was counted in 5 fields in each section by two independent observers using a light microscope or a fluorescence microscope (10 × 40) as another previous study shown 19.

Cell transfection

Chondrocytes transfected with miR-15b mimics, inhibitor, negative control, inhibitor negative control or siRNA (50 nM) (GenePharma, Shanghai, China) by GenMuteTM siRNA & DNA Transfection Reagent (SignaGen, Rockville, MD, USA) according to manufacturer's protocols. The sequences were as follows: miR-15b mimics: 5′-UAGCAGCACAUCAUGGUUUACA-3′, 5′-UAAACCAUGAUGUGCUGCUAUU-3′; miR-15b inhibitor: 5′-UGUAAACCAUGAUGUGCUGCUA-3′; MircroRNA negative control: 5′-UUCUCCGAACGUGUCACGUTT-3′, 5′-ACGUGACACGUUCGGAGAATT-3′; IGF1 siRNA: 5′-GCACGAGUUACCUGUUAAATT-3′, 5′-UUUAACAGGUAACUCGUGCTT-3′; To find the best concentration of miR-15b mimics, inhibitor or negative control, different groups of chondrocytes were divided as 0 nM, 10 nM, 30 nM, 50 nM and 80 nM. The optimal concentration of miR-15b mimics, inhibitor or negative control was 50 nM. The transfection efficiency was estimated using 5-carboxyfluorescein-connected miRNA negative control at 6–8 h after transfection under a fluorescence microscope. The percentage of transfected cells with fluorescence was about 70–80%.

Luciferase report assay

The reporter plasmid containing 485bp of the 3' -untranslated regions (3′-UTR) of human IGF1 mRNA, 487bp of the 3' -untranslated regions (3′-UTR) of human IGF1R mRNA or 482bp of the 3′-untranslated regions (3′-UTR) of human BCL2 mRNA was constructed by the p-EZX-MT01 miRNA expression reporter vector

system (GeneCopoeia, USA). The nucleotide sequence complementary of mature miR15b-5p seed sequence (ACAUUUGGUACUACACGACGAU) was included in three reporter plasmids. The nucleotide sequence complementary to miR15b-5p was changed in the mutant plasmid. The 3′-UTR of integrated with firefly luciferase (hLuc) and the internal reference was renilla luciferase (hRLuc). Chondrocytes transfected with 0.5μg of reporter plasmid and 50 nM miRNA mimics or negative control using GenMute (SignaGen, USA) according to manufacturer's protocols in every single well of 6-well plate. The transfection efficiency was maintained at a level around 80% by fluorescence observation in control group, which was shown in Appendix 2. After 48 h of transfection, luciferase activity assay was carried out by Luc-Pair ™ Duo-Luciferase Assay Kit 2.0 (GeneCopoeia, USA) and using GloMax 20/20 LUMINOMETER (promega, USA) to measure fluorescence. Firefly luciferase activity was normalized to Renilla luciferase activity.

Proliferation Assay (cell cycle Assay and cck8)

When the percentage of cell reached about 80%, cells were washed with PBS twice. Digested the cells by 0.25% trypsin, then seeded the cells to a 96-well plate with 3 × 103-6 × 103 cells in each well. Cells were cultured in an incubator with six repeated wells. After 48 h, the plates were taken out and then 10 μL CCK8 (DOJINDO, JAPAN) was added for 2 h of culture. EL-301 enzyme linked immunosorbent assay (Omega Bio-Tek Inc., Norcross, GA, USA) was used to read optical density (OD) value at 450 nm. 3 times repeated in each procedure.

After being transfected for 48 h, chondrocytes were collected and pre-cooled at −200C of 75% ethanol was used to fix cells overnight at 40C. After the ethanol and the supernatant of PBS were discarded, the addition of RNase was performed in the dark. Then cells were being put in the water bath in the dark for 30 min. And then stained the cells with propidium iodide (PI) (Sigma–Aldrich Chemical Company, St Louis, MO, USA) for 30 min in the dark at 40C, cell cycle stages were detected and red fluorescence was recorded by flow cytometry (Beckman, USA). Three times of repetition of each experiment was performed. Results were presented as percentage of cell in a particular phase.

Apoptosis assay

Cell apoptosis analysis was performed according to the manufacturer's instructions by Annexin-VFITC Apoptosis Detection Kit (BD, USA). Chondrocytes were transfected with miR-15b-5p mimics, miR-15b-5p inhibitor and miR-15b-5p negative control when the percentage of cells grown to 70–90%. After transfection, cells were incubated at 37°C for 48 h. Then the Annexin V/fluorescein isothiocyanate Apoptosis Detection kit was used to stain the cells. Cell apoptosis was detected using a flow cytometer (Beckman, USA) and the percentage was measured by the software of ModFit.

Hoechst 33,342 (Beyotime Institute of Biotechnology, Jiangsu, China) staining was used to assess apoptotic chondrocytes in quantitative assessment according to the manufacturer's instructions, and fluorescence microscope (Leica, Wetzlar, Germany) used to count the positive cells.

Statistical analysis

All data were analyzed using Prism 5.0 (Graphpad software, San Diego, California, USA). All quantitative data were presented as the means and 95% confidence intervals (CIs). Non-parametric Mann–Whitney *U* test was used for two independent groups. For the data of luciferase report assay, one-way analysis of variance (ANOVA) with Tukey's *post hoc* analysis was used for multi-comparisons after confirmation of data fulfilling normal distribution and homogeneity of variances. $P < 0.05$ was considered statistically significant.

Appendix 2. The transfection efficiency was maintained at a level around 80% by fluorescence observation in control group

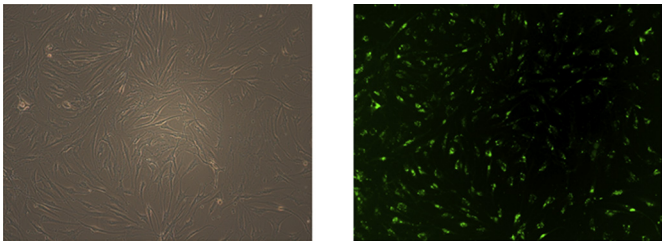

Appendix 3. The protein level of IGF1 evidently decreased after transfection of IGF1 siRNA

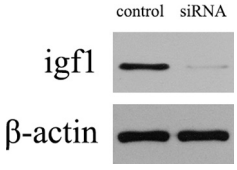

References

1. Chen Y, Ke J, Long X, Meng Q, Deng M, Fang W, *et al.* Insulin-like growth factor-1 boosts the developing process of condylar hyperplasia by stimulating chondrocytes proliferation. Osteoarthritis Cartilage Apr 2012;20(4):279–87.
2. Gotz W, Lehmann TS, Appel TR, Rath-Deschner B, Dettmeyer R, Luder HU, *et al.* Distribution of insulin-like growth factors in condylar hyperplasia. Ann Anat Anatomischer Anzeiger 2007;189(4):347–9.
3. Verhoeven TJ, Nolte JW, Maal TJ, Berge SJ, Becking AG. Unilateral condylar hyperplasia: a 3-dimensional quantification of asymmetry. PLoS One 2013;8(3):e59391.
4. Meng Q, Long X, Deng M, Cai H, Li J. The expressions of IGF-1, BMP-2 and TGF-beta 1 in cartilage of condylar hyperplasia. J Oral Rehabil Jan 2011;38(1):34–40.
5. Xue X, Zhang J, Lan H, Xu Y, Wang H. Kaiso protects human umbilical vein endothelial cells against apoptosis by differentially regulating the expression of B-cell CLL/lymphoma 2 family members. Sci Rep Aug 2 2017;7(1):7116.
6. Wojtuszkiewicz A, Schuurhuis GJ, Kessler FL, Piersma SR, Knol JC, Pham TV, *et al.* Exosomes secreted by apoptosis-resistant acute myeloid leukemia (AML) blasts harbor regulatory network proteins potentially involved in antagonism of apoptosis. Mol Cell Proteomics Apr 2016;15(4):1281–98.
7. Liu S, Yang H, Hu B, Zhang M. Sirt1 regulates apoptosis and extracellular matrix degradation in resveratrol-treated osteoarthritis chondrocytes via the Wnt/beta-catenin signaling pathways. Exp Ther Med Nov 2017;14(5):5057–62.
8. Jacobson MD, Burne JF, King MP, Miyashita T, Reed JC, Raff MC. Bcl-2 blocks apoptosis in cells lacking mitochondrial DNA. Nature Jan 28 1993;361(6410):365–9.
9. Pekarsky Y, Balatti V, Croce CM. BCL2 and miR-15/16: from gene discovery to treatment. Cell Death Differ Jan 2018;25(1):21–6.
10. Chipuk JE, Moldoveanu T, Llambi F, Parsons MJ, Green DR. The BCL-2 family reunion. Mol cell Feb 12 2010;37(3):299–310.

11. Vimalraj S, Selvamurugan N. Regulation of proliferation and apoptosis in human osteoblastic cells by microRNA-15b. Int J Biol Macromol Aug 2015;79:490–7.
12. Luan X, Zhou X, Trombetta-eSilva J, Francis M, Gaharwar AK, Atsawasuwan P, *et al.* MicroRNAs and periodontal homeostasis. J Dent Res May 2017;96(5):491–500.
13. Xu J, Liu Y, Deng M, Li J, Cai H, Meng Q, *et al.* MicroRNA221-3p modulates Ets-1 expression in synovial fibroblasts from patients with osteoarthritis of temporomandibular joint. Osteoarthritis Cartilage Nov 2016;24(11):2003–11.
14. Tao L, Li X, Han NN, Zhou Q, Liu ZL. MicroRNA-497 accelerates apoptosis while inhibiting proliferation, migration, and invasion through negative regulation of the MAPK/ERK signaling pathway via RAF-1. J Cell Physiol Oct 2018;233(10):6578–88.
15. Wu DM, Zhang YT, Lu J, Zheng YL. Effects of microRNA-129 and its target gene c-Fos on proliferation and apoptosis of hippocampal neurons in rats with epilepsy via the MAPK signaling pathway. J Cell Physiol Sep 2018;233(9):6632–43.
16. Huang Z, Zhang N, Ma W, Dai X, Liu J. MiR-337-3p promotes chondrocytes proliferation and inhibits apoptosis by regulating PTEN/AKT axis in osteoarthritis. Biomed Pharmacother Biomedecine Pharmacotherapie Nov 2017;95:1194–200.
17. Wu YH, Liu W, Zhang L, Liu XY, Wang Y, Xue B, *et al.* Effects of microRNA-24 targeting C-myc on apoptosis, proliferation, and cytokine expressions in chondrocytes of rats with osteoarthritis via MAPK signaling pathway. J Cell Biochem Nov 2018;119(10):7944–58.
18. Lopez DF, Lopez C, Moreno M, Pinedo R. Post-condylectomy histopathologic findings in patients with a positive (99m)Tc methylene diphosphonate single-photon emission computed tomographic diagnosis for condylar hyperplasia. J Oral Maxillofac Surg Off J Am Assoc Oral Maxillofac Surg May 2018;76(5):1005–12.
19. Luo HJ, Li YT, Liu B, Yang YT, Xu ZQD. MicroRNA-15b-5p targets ERK1 to regulate proliferation and apoptosis in rat PC12 cells. Biomed Pharmacother Aug 2017;92:1023–9.
20. Xiao JS, Liu L, Zhong ZA, Xiao C, Zhang JJ. Mangiferin regulates proliferation and apoptosis in glioma cells by induction of microRNA-15b and inhibition of MMP-9 expression. Oncol Rep Jun 2015;33(6):2815–20.
21. Sun G, Shi L, Yan SS, Wan ZQ, Jiang N, Fu LS, *et al.* MiR-15b targets cyclin D1 to regulate proliferation and apoptosis in glioma cells. BioMed Res Int 2014:687826.
22. Satzger I, Mattern A, Kuettler U, Weinspach D, Voelker B, Kapp A, *et al.* MicroRNA-15b represents an independent prognostic parameter and is correlated with tumor cell proliferation and apoptosis in malignant melanoma. Int J Cancer Jun 2010;126(11):2553–62.
23. Shen J, Wan R, Hu GY, Yang LJ, Xiong J, Wang F, *et al.* miR-15b and miR-16 induce the apoptosis of rat activated pancreatic stellate cells by targeting Bcl-2 in vitro. Pancreatology Mar-Apr 2012;12(2):91–9.
24. Saglam ASY, Alp E, Elmazoglu Z, Menevse S. Treatment with cucurbitacin B alone and in combination with gefitinib induces cell cycle inhibition and apoptosis via EGFR and JAK/STAT pathway in human colorectal cancer cell lines. Hum Exp Toxicol May 2016;35(5):526–43.
25. Li ZJ, Pan WH, Shen Y, Chen ZL, Zhang LH, Zhang YP, *et al.* IGF1/IGF1R and microRNA let-7e down-regulate each other and modulate proliferation and migration of colorectal cancer cells. Cell Cycle 2018;17(10):1212–9.
26. Guo CJ, Pan Q, Li DG, Sun H, Liu BW. miR-15b and miR-16 are implicated in activation of the rat hepatic stellate cell: an essential role for apoptosis. J Hepatol Apr 2009;50(4):766–78.
27. Porter AG, Janicke RU. Emerging roles of caspase-3 in apoptosis. Cell Death Differ Feb 1999;6(2):99–104.
28. Volpe E, Sambucci M, Battistini L, Borsellino G. Fas-fas ligand: checkpoint of T cell functions in multiple sclerosis. Front Immunol 2016;7:382.
29. Wu S, Fadoju D, Rezvani G, De Luca F. Stimulatory effects of insulin-like growth factor-I on growth plate chondrogenesis are mediated by nuclear factor-kappaB p65. J Biol Chem Dec 5 2008;283(49):34037–44.
30. Yu S, Sun L, Liu L, Jiao K, Wang M. Differential expression of IGF1, IGFR1 and IGFBP3 in mandibular condylar cartilage between male and female rats applied with malocclusion. J Oral Rehabil Oct 2012;39(10):727–36.
31. Kinkel MD, Yagi R, McBurney D, Nugent A, Horton Jr WE. Age-related expression patterns of Bag-1 and Bcl-2 in growth plate and articular chondrocytes. Anat Rec Part A, Discoveries in molecular, cellular, and evolutionary biology Aug 2004;279(2):720–8.
32. Zhao C, Wang GY, Zhu YY, Li XB, Yan FH, Zhang CH, *et al.* Aberrant regulation of miR-15b in human malignant tumors and its effects on the hallmarks of cancer. Tumor Biol Jan 2016;37(1):177–83.
33. Lovat F, Fassan M, Gasparini P, Rizzotto L, Cascione L, Pizzi M, *et al.* miR-15b/16-2 deletion promotes B-cell malignancies. Proc Natl Acad Sci USA Sep 2015;112(37):11636–41.
34. MacLean II JA, King ML, Okuda H, Hayashi K. WNT7A regulation by miR-15b in ovarian cancer. PLoS One May 19 2016;11(5).
35. Park HJ, Kim MJ, Ha E, Chung JH. Apoptotic effect of hesperidin through caspase 3 activation in human colon cancer cells, SNU-C4. Phytomedicine Jan 2008;15(1–2):147–51.
36. Saini U, Gumina RJ, Wolfe B, Kuppusamy ML, Kuppusamy P, Boudoulas KD. Preconditioning mesenchymal stem cells with caspase inhibition and hyperoxia prior to hypoxia exposure increases cell proliferation. J Cell Biochem Nov 2013;114(11):2612–23.
37. Sun HJ, Meng XZ, Han JH, Zhang Z, Wang B, Bai XD, *et al.* Anti-cancer activity of DHA on gastric cancer-an in vitro and in vivo study. Tumor Biol Dec 2013;34(6):3791–800.
38. Chen R, Sheng L, Zhang HJ, Ji M, Qian WQ. miR-15b-5p facilitates the tumorigenicity by targeting RECK and predicts tumour recurrence in prostate cancer. J Cell Mol Med Mar 2018;22(3):1855–63.
39. Xiao J, Cao YL, Fan HH. Apoptosis of fetus chondrocytes cultured in vitro and expression of caspase-3. Zhongguo Xiu Fu Chong Jian Wai Ke Za Zhi Sep 2003;17(5):418–21.
40. Hwang HS, Park SJ, Lee MH, Kim HA. MicroRNA-365 regulates IL-1 beta-induced catabolic factor expression by targeting HIF-2 alpha in primary chondrocytes. Sci Rep Dec 20 2017;7(1):17889.